Dependence of film tension on the thickness of smectic films

R. Jaquet and F. Schneider
Theoretische und Physikalische Chemie, Universität Siegen, 57068 Siegen, Germany
(Received 26 September 2002; published 26 February 2003; publisher error corrected 25 August 2003)

The film tension τ of free standing S_A films has been measured for films with thicknesses between 2 and 150 layers. There is a clear increase of τ with the thickness for very thin films and a nonlinear slower increase for high thickness. The nonlinearity depends on the amount of liquid crystal accessible to the meniscus of the film during the drawing process. Several models are discussed that describe these effects.

DOI: 10.1103/PhysRevE.67.021707 PACS number(s): 61.30.−v, 68.03.Cd, 68.60.Bs

I. INTRODUCTION

Free standing smectic films can be produced with constant thickness over large areas. Directly after the drawing process the thickness is usually not constant. Thin areas begin to grow at the expense of thick areas until the thinnest part has spread over the whole film area. This phenomenon can only be explained if the film tension increases with the film thickness D.

The film tension $\tau=(\partial G/\partial A)_{p,T}$ (G, free enthalpy, A, film area) contains two terms. One is the double surface tension σ and the second is due to the pressure difference $\Delta p = p_{film} - p_{env}$ [1–3] between film and environment

$$\tau = 2\sigma - \Delta p\, D. \tag{1}$$

The pressure difference is caused by the concave meniscus as described by the equation of Young and Laplace, and is therefore negative.

Besides the increase of film tension as described by Eq. (1), there must be an additional effect in ultrathin films in which disclinations between regions with different thicknesses move very rapidly. Thus a two layer film is formed nearly instantaneously from a film with a two layer region and thicker regions. In several studies [4–6] Landau models have been developed predicting a decrease of film tension in ultrathin films.

All measurements up to now have not observed the increase of film tension with the film thickness [7–12] except one study [1] at very thick films (4000–8000 layers). Recently, one of us (F.S.) has described a new method [13] for the measurement of film tension, which gives very precise results and should be able to detect this effect.

II. EXPERIMENTAL METHOD

The measurements were performed with the liquid crystal *n*-octyl-cyano-biphenyl (8CB), which exhibits an S_A phase between 21.0 and 33.0 °C. The liquid crystal was purchased from Synthon GmbH, Wolfen and used without further purification.

The film tension is determined from the force of a film drawn between two circular edges (two ring method, see Fig. 1). The upper edge is suspended from an electronic balance with a resolution of 10^{-5} g. As the force of the film corresponds to about 2 g, the relative resolution of the device is 5×10^{-6}. The details of the experimental setup have been reported elsewhere [13].

A minor modification in the setup has been introduced in order to simplify the drawing of thick films. Thick films are formed if the opening velocity of the edges is small. In the new setup the upper ring can be moved upward by means of a plate, which is inserted between the rings. The movement of the upper plate is therefore strictly parallel to the lower ring. Finally, the lower ring and the plate are moved downward, until the upper ring is suspended from the balance and the film exhibits the height desired. In the old setup the lower edge was moved downward from the beginning and the opening of the edges occurred asymmetrically. This led to a mechanical instability and a subsequent wobbling of the upper ring when the edges were separated from one another.

The thickness of thin films with 2 to 20 smectic layers was determined by means of the reflectivity of light at a fixed wavelength of 635 nm generated by an interference filter from white light (100 W halogen lamp, Xenophot, Osram). The method of measurement and the evaluation have been described in several papers [14,15].

The thickness of thick films was determined from the interference spectra of the reflected beam in the visible region [16]. Figure 2 shows the optical setup.

Evaluation of the interference spectra of smectic films is simple if the film is illuminated with light parallel to the film normal. Due to the two-dimensional bending of the film a

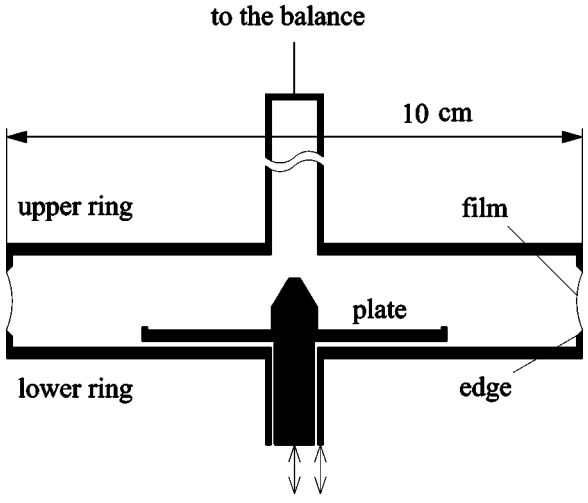

FIG. 1. Schematic diagram of the setup.

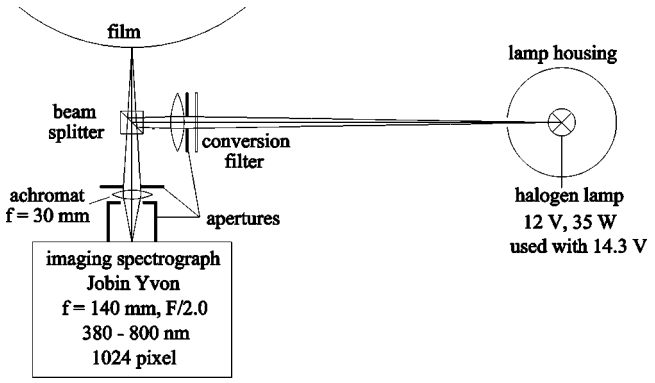

FIG. 2. Optical setup.

broad parallel beam of light is unfavorable. The filament (6×1.5 mm) of the halogen lamp is therefore imaged on the film with a maximum deviation from normal incidence of 2°. The conversion filter (Linos, TL60) reduces the light intensity at the wavelength of the maximum signal of the imaging spectrograph (520 nm) and transmits the light at short and long wavelengths. After calibration with 20 spectral lines between 378 nm (Tl) and 770 nm (K) the precision of the wavelength determination of the interference spectra is 0.1 nm.

For normal incidence the reflected intensity I is

$$\frac{I}{I_0}=\frac{4R\sin^2(\delta/2)}{(1-R)^2+4R\sin^2(\delta/2)}, \tag{2}$$

where $\delta=4\pi n_o D/\lambda$ and $R=(n_o-1)^2/(n_o+1)^2$. n_o is the ordinary refractive index of the smectic liquid crystal. Unfortunately the refractive indices of 8CB are not known as a function of wavelength. Wu *et al.* [17] have measured the indices for the pentyl homologue of 8CB in the nematic phase. Due to the different alkyl chain lengths, different phases, and different temperatures the indices at 589 nm are slightly different (1 %). This was taken into account as follows. The indices of Wu *et al.* were described by a three-band Sellmeier equation

$$n_o=1+g_0+g_1\frac{\lambda^2\lambda_1^2}{\lambda^2-\lambda_1^2}+g_2\frac{\lambda^2\lambda_2^2}{\lambda^2-\lambda_2^2}, \tag{3}$$

with the λ_i values 210 and 282 nm [17]. The coefficients g_i were changed linearly such that the refractive index at 589 nm agreed with the measured value of 8CB.

The measuring system had to be calibrated for the determination of the reflected intensity from the output of the imaging spectrograph. In principle, the calibration can be performed by measuring the reflected intensity of a surface with known reflectivity, e.g., a glass plate. However, the calibration curve $I_c(\lambda)$ strongly depends on position, orientation, and bending of the reflecting surface. The simplest method was to measure the reflected intensity of a thin film itself. For very thin films up to about five smectic layers Eq. (2) can be expanded to give

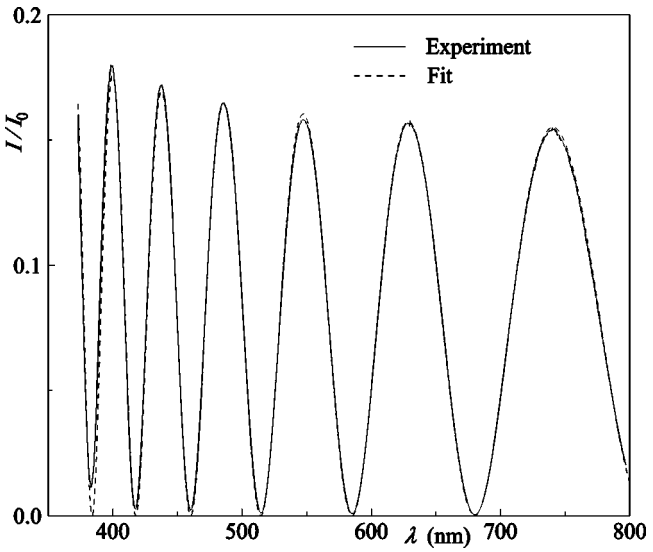

FIG. 3. Experimental interference spectrum and fit of a thick film at 21.9 °C.

$$\frac{I}{I_0}=\pi^2(n_o^2-1)^2\frac{D^2}{\lambda^2}. \tag{4}$$

A calibration with an interference spectrum of such a thin film does not require the knowledge the film thickness D if only relative intensities are to be determined.

Calibration with thicker films, e.g., with eight smectic layers, gives higher intensities. In this case Eq. (2) has to be used and the film thickness has to be known. As the layer thickness d is known from x-ray measurements [18] or from the interference spectra (see below) only some integer layer numbers N have to be tested. For wrong values the calibration procedure leads to wrong maximum intensities in the interference spectra of thick films. Therefore, the layer number and the film thickness $D=Nd$ can be determined unambiguously.

Figure 3 shows the interference spectrum of a thick 8CB film and a fit with Eq. (2) with $D=1352.5$ nm. For wavelengths longer than 450 nm the fit is nearly perfect. For smaller wavelengths the refractive indices are obviously incorrect and the intensities at the minimum and maximum values are too high. The last effect is probably caused by the scattering of light from the smectic film and an insufficient resolution of the spectrograph. By means of the fit the film thickness could be determined with an error of 0.1 to 0.2 nm for films between about 40 and 200 layers.

Table I shows a series of measured film thicknesses, which were determined at two different days. From these measurements the layer thickness can be determined as the minimum of the function

$$\Delta=\frac{\sum_{i=1}^{M}[D_i/d-\mathcal{I}_{\mathrm{near}}(D_i/d)]^2}{M}. \tag{5}$$

TABLE I. Measured film thickness D for 8CB at 21.9 °C and number N of smectic layers.

D/nm	N
132.0	42.08
156.7	49.96
163.1	52.00
166.2	52.99
172.5	54.99
175.6	55.98
178.8	57.00
219.5	69.98
232.1	73.99
235.2	74.98
247.9	79.03
247.9	79.03
254.1	81.01
297.9	94.97
338.9	108.04
367.1	117.03
370.2	118.02
379.7	121.05
382.8	122.04
382.8	122.04
401.3	127.94
401.3	127.94
429.9	137.05
442.0	140.91
442.2	140.98

The index i runs over the M measured values. d is the variable layer thickness and $\mathcal{I}_{\text{near}}$ means ''nearest integer.'' Figure 4 shows the function Δ for the interesting thickness region. The global minimum is at 3.137 nm, which is in good agreement with the x-ray value from Leadbetter *et al.* [18] of 3.16 nm. Table I shows that the calculated layer numbers are nearly integer values and that the corresponding layer numbers can be determined exactly in this range of film thicknesses.

III. EXPERIMENTAL RESULTS

A. Thin films

Within this experiment the films were drawn and destroyed after every measurement. Therefore it was possible to determine the balance readings without film and to calibrate the light intensity after every measurement. The drawing technique only allows to define a broad range of thicknesses for the films to be prepared. Therefore, and due to the limited number of experiments during one series of measurements, some layers are missing in each series in Fig. 5, showing the measurements for 8CB at several temperatures.

For films with more than eight layers the film tension achieves aconstant value. Equation (1) predicts a linear dependence on the film thickness for a constant pressure difference. For small D values the contribution of the second term is very small and is not observed. For thinner films a decrease is observed as found for other liquid crystals, too. A simple argument for the decrease is the following. The surface tension corresponds to the free enthalpy, which is necessary to create a definite film surface. The liquid crystal material needed for the additional film area has to be pulled out of the meniscus. The properties of the bulk material in the meniscus and the material in the inner part of a thick film agree with one another, i.e., the excess of the free enthalpy of a film is only caused by the outer layers with its higher enthalpy density. For very thin films the order parameters in the outer layers increase due to the interaction of the two highly ordered surfaces. This leads to a decrease of the free enthalpy density and the surface tension.

A more detailed discussion of this effect is presented in Sec. IV.

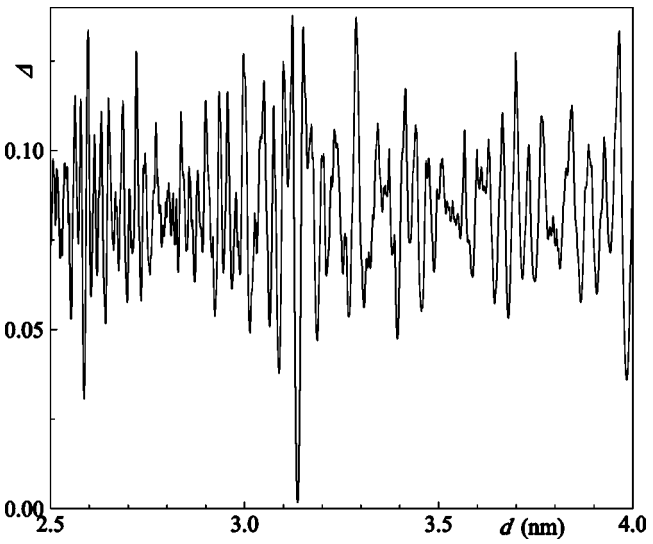

FIG. 4. Function Δ [Eq. (5)] versus layer thickness d.

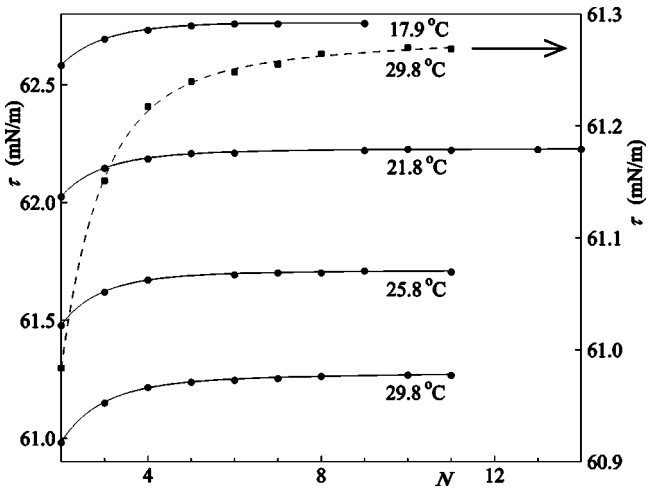

FIG. 5. Film tension τ versus layer number N at temperatures between 17.9 and 29.8 °C. The solid lines are only guides for the eye. Additionally, the measurement at 29.8 °C is presented at a higher resolution.

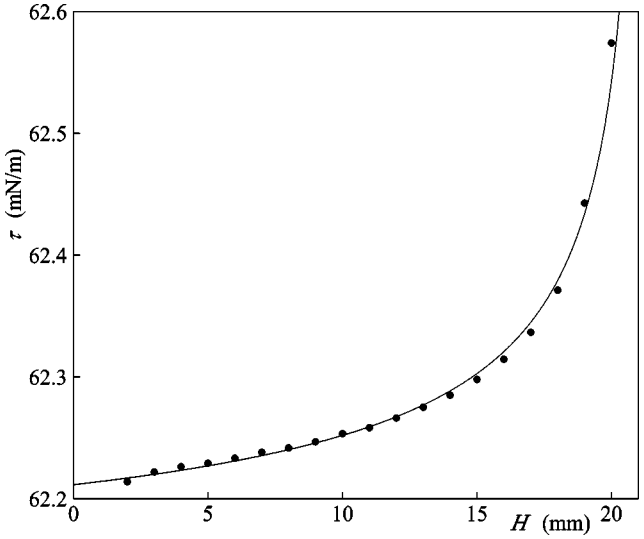

FIG. 6. Film tension τ versus film height H for a 100 layer film at 21.9 °C. The solid line is calculated with Eqs. (1) and (9).

B. Thick films

In thick films the surfaces are well separated, leading to a negligible interaction between molecules in the two surfaces and no change of the film tension. However, the second term in Eq. (1) predicts an increase of τ with the film thickness. Whether this increase is linear in the thickness [1] or not has to be investigated. The pressure difference

$$\Delta p = \frac{\sigma}{r_m} \tag{6}$$

is a function of the curvature radius $r_m < 0$ of the meniscus and should depend on the available amount of liquid crystal, the film volume, and the length of the meniscus.

Figure 6 shows the film tension τ as a function of the film height. The evaluation of the measurement takes into account [13] that the film does not exhibit the form of a cylinder, but that of a minimum surface between two circular edges. No change of the film tension [see Eq. (1)] is expected if the curvature radius of the meniscus and correspondingly the pressure difference remain constant.

The amount of liquid crystal for the film has to be provided by the menisci. This leads to a decrease of the curvature radius, as observed experimentally during the drawing process. In our experiment the material flow is about 2 mg for a film with a height of 20 mm and a thickness of 100 layers.

A simple model allows to determine the curvature radius from film height and thickness. The cross section of the meniscus is represented by the area between the edge, which is assumed to be circular, and the circular surface of the meniscus (Fig. 7).

The volume of the upper and lower meniscus is obtained as

$$V_m = 4\pi R(|r_m|\sqrt{r_e^2 + 2r_e|r_m|} - \alpha r_e^2 - \beta r_m^2) \tag{7}$$

with

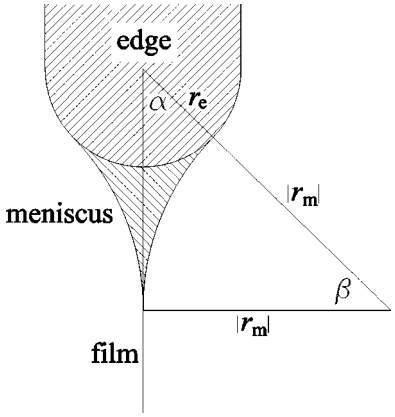

FIG. 7. Simple model for the cross section of the menisci. The true form of the edge is a 45° trapezoid with a thickness of 1 mm.

$$\sin\alpha = \frac{|r_m|}{r_e + |r_m|} \quad \text{and} \quad \alpha + \beta = \pi/2. \tag{8}$$

R is the diameter of the circular edge (10 cm). The liquid crystal volume V_{LC} in the menisci and in the film becomes

$$V_{LC} = 2\pi R(2|r_m|\sqrt{r_e^2 + 2r_e|r_m|} - 2\alpha r_e^2 - 2\beta r_m^2 + HD) \tag{9}$$

for $H \gg |r_m|\tan\beta - r_e$. For the further evaluation the quantities $V_{LC}/2\pi R$ and r_e are assumed to be free selectable parameters. Equation (9) is solved numerically for r_m with given values for the film thickness D, and the film tension is calculated with Eq. (1). The edge radius r_e has only a minor influence on the form of the calculated curve shown in Fig. 6. τ is calculated with the fit parameters $V_{LC}/2\pi R = 6.7 \times 10^{-3}$ mm^2, $r_e = 0.3$ mm, and $\sigma = 31.062$ mN m^{-1}, which exhibit the correct order of magnitude.

The determination of the film tension is influenced by the weight of the film (2 mg for the full height). One half of the film material stems in a first approximation from the upper meniscus; however, the full film is suspended from the upper ring. Furthermore, the weight of the film must be compensated by a slightly smaller radius of the curvature of the upper meniscus, i.e., more than one half of the film material comes from the upper meniscus. The error in the determination of the film tension corresponds to less than one half of the weight of the film. Altogether this leads to an error of the film tension of about 0.02 mN m^{-1} at the largest film height.

In the next experiment the height of the film was kept constant (10 mm) and the thickness was changed. If the film is destroyed after every measurement and the new film is drawn after a contact of the edges the scattering of the values becomes very strong. Obviously, this is a consequence of different liquid crystal volumes in the menisci. The scattering can be reduced if one avoids destruction of the film during one series of measurements. As a consequence, a balance calibration between the measurements cannot be performed. This is no drawback for our device, with its very good long time stability [13]. Different film thicknesses are obtained by rapid compressions and expansions of the film area.

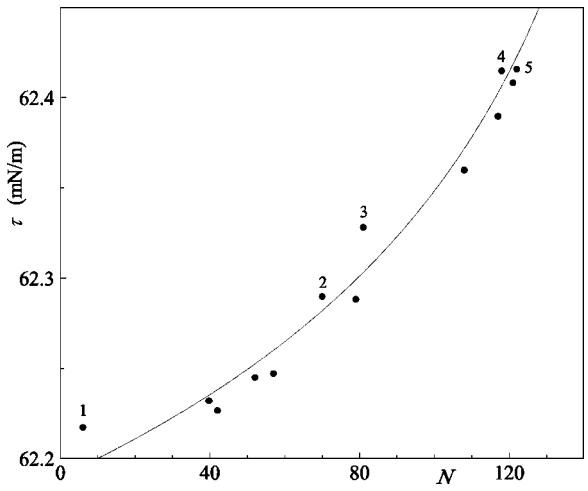

FIG. 8. Film tension τ versus layer number N for thick films with constant height at 21.9 °C. The numbers at the measured values show the sequence of measurements. The solid line is calculated with Eqs. (1) and (9).

The result is shown in Fig. 8. There is a clear influence of the time of measurement on the deviation of the values from the mean curve. Early measurements result in values above the mean curve. The reason for this effect is the following. The first film with a large thickness sucks liquid crystal material from more distant parts of the edge into the meniscus. After this irreversible process the material is now accessible when thin films are drawn. This process reduces the weight of the upper ring with the adhering liquid crystal and increases the curvature radius of the menisci. Both effects result in an apparent reduction of the film tension.

The simple model introduced above can also be applied to this experiment. The solid line in Fig. 8 was calculated with the parameters $V_{LC}/2\pi R = 5.6\times10^{-3}$ mm^2, $r_e = 0.3$ mm, and $\sigma = 31.095$ mN m^{-1}, which agree reasonably with the parameters used for the fit in Fig. 6.

IV. MODEL FOR THE SURFACE TENSION IN THIN FILMS

In ultrathin smectic films pseudo van der Waals interactions arise from the decrease of orientational and positional fluctuations [4,19,20]. The influence on the film tension is in the order of

$$\Delta\tau = -\frac{A}{12\pi D^2}, \tag{10}$$

where $A \approx 10\ kT$ is the Hamaker constant. For a two layer film this effect gives only 10% of the observed decrease and the predicted $1/D^2$ dependence is not observed.

Picano *et al.* [4] have studied the interaction of the two surfaces of a smectic film with a Landau–de Gennes model and find a decrease of the film tension $\Delta\tau$ for very thin films:

$$\Delta\tau = \frac{a\xi\psi_s^2}{\sqrt{2}}[1-\tanh(Nd/\sqrt{2}\xi)] \tag{11}$$

with

$$a = a_0(T - T_{NA}), \tag{12}$$

$$\xi = \xi_0[(T_{NA}-T)/T_{NA}]^{-1/2}, \quad T < T_{NA}, \tag{13}$$

ψ_s, the excess of the smectic order parameter at the free surface, is assumed to be constant. Picano *et al.* [4] propose the values $a_0\xi_0\psi_s^2/\sigma = 7.4\times10^{-4}$ K^{-1} and $\xi_0 = 0.8$ nm for 8CB from their measurements of the meniscus profile. This already leads to a nearly correct description of the decrease of τ in thin films.

For the further study we have subtracted from the experimental values a linear dependence on D (0.001 mN/m$\times N$) resulting from the approximately linear term $\Delta p\, D$ in Eq. (1). Furthermore, $\Delta\tau$ was determined by subtracting the constant τ of the thick films.

For constant temperature Eq. (11) can be written as

$$\Delta\tau = K[1-\tanh(Nd/l)] \tag{14}$$

and allows a fit within the experimental error.

Figure 9 shows that the temperature dependence of $\Delta\tau$ is not well described by Eq. (11).

In the experiment the onset of the decrease of τ does not depend on the temperature. Function (11), however, moves this with temperature. This problem of the theory has already been observed by Picano *et al.* [4] in their study of the contact angle between film and meniscus.

Improved theories by Shalaginov and Sullivan [5] and Poniewierski *et al.* [6] take into account the quartic term of the Landau–de Gennes theory and use a better description of the surface energy. The dependence of the Landau free energy on the phase ϕ of the smectic order parameter $\Psi = \psi\exp(i\phi)$ can be neglected in the smectic phase. Then the Landau free energy functional per area has the following form:

$$f(\psi) = 2\int_0^{D/2}\left[\frac{1}{2}L\left(\frac{d\psi}{dz}\right)^2 + \frac{a}{2}\psi^2 + \frac{b}{4}\psi^4\right]dz + 2\left[-h_s\psi(D/2) + \frac{g_s}{2}\psi^2(D/2)\right]. \tag{15}$$

ψ is the amplitude of the smectic order parameter. The solution of the functional leads to the Euler-Lagrange equation

$$L\frac{d^2\psi}{dz^2} - a\psi - b\psi^3 = 0 \tag{16}$$

with the boundary conditions

$$\frac{d\psi}{dz}(0) = 0, \tag{17}$$

$$L\frac{d\psi}{dz}(D/2) = h_s - g_s\psi(D/2). \tag{18}$$

L, $a = a_0(T_{NA}-T)$, b, h_s, and g_s are the phenomenological parameters of the model.

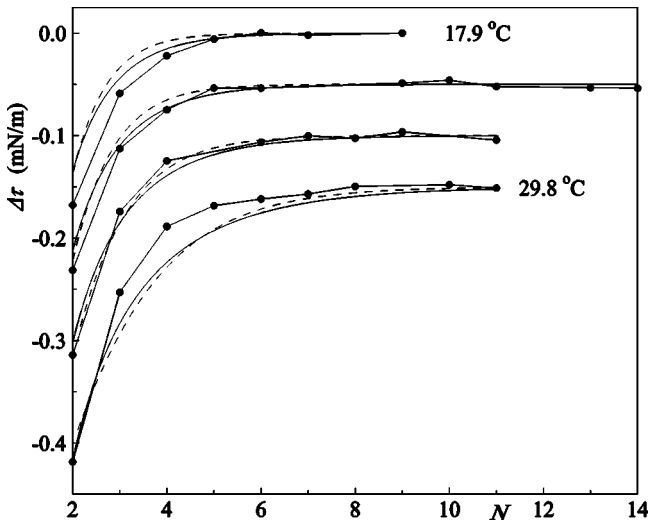

FIG. 9. Film tension decrease $\Delta\tau$ versus layer number N for thin films at different temperatures and fit (– – – –) with Eq. (11) with the parameters $a_0\xi_0\psi_s^2/\sqrt{2}=1.92\times10^{-5}$ N/mK and $d/(\sqrt{2}\xi_0)=3.256$. The solid lines are a fit with an improved Landau–de Gennes theory [5,6] (see below). The curves have been shifted for clarity.

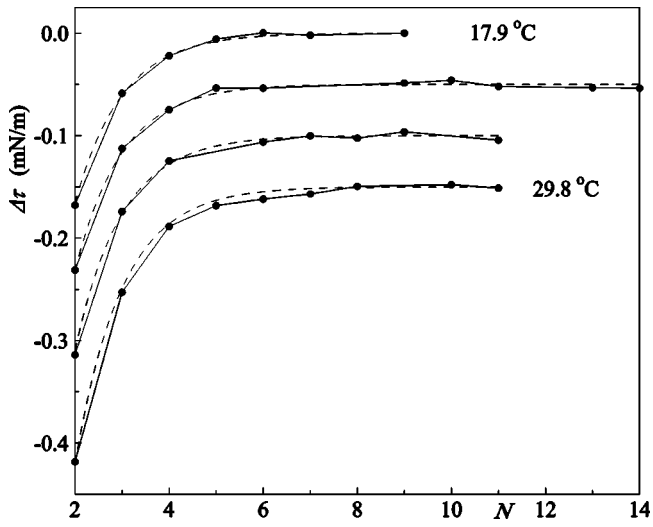

FIG. 10. Film tension decrease $\Delta\tau$ versus layer number N for thin films at different temperatures and fit (– – – –) with Eq. (21).

The contribution of the smectic order to the film tension corresponds to the difference between the Landau free energy of the film and the bulk:

$$f(\psi_{eq})-f(\psi_{b,eq})=\tau_{sm}. \tag{19}$$

Finally, $\Delta\tau$ is obtained from the τ_{sm} values for films with finite and infinite thickness

$$\Delta\tau=\tau_{sm}(D)-\tau_{sm}(\infty). \tag{20}$$

The differential equation has been solved using the shooting method [21]. With $h_s=0$ and reasonable values for the ratio $L/a=-\xi^2$ we found the best fit for $L/bd^2=2$, $a_0/b=0.07$, $g_s/bd=-0.3$, and $bd=0.01$ N/m. There is a minor improvement (see Fig. 9, solid lines) compared with the fit based on the simple theory. Especially, the error in the temperature dependence is not reduced significantly.

In both theories the decrease of the surface order with the distance from the surface is described by the coherence length ξ. For a cell thickness of about 2ξ the decrease of τ begins. The experiment shows no clear dependence of this beginning as a function of temperature, whereas Eq. (13) predicts a temperature dependence.

The experimental observation suggests to eliminate this temperature dependence with a phenomenological ansatz of the form

$$\Delta\tau=K/(T_{NA}-T)^{\kappa}\exp(-Nd/l). \tag{21}$$

The whole set of data can be described with $K=2.936\times10^{-3}$ N/m, $\kappa=0.316$, and $d/l=1.007$ within the experimental error (see Fig. 10).

V. CONCLUDING REMARKS

In contrast to earlier studies [7–12] we have found a clear dependence of the film tension on the film thickness. The negative pressure difference between film and surrounding gas leads to a nonlinear increase of the film tension with the film thickness. Furthermore, we have observed an increase of the film tension with the film area. This effect is due to the limited amount of liquid crystal in the meniscus. An increase of the film area requires liquid crystal material that leads to a decrease of the curvature radius of the meniscus and an increase of the pressure difference.

In addition, ultrathin liquid crystal films with a thickness of $N=2$–4 smectic layers show an increase of the film tension with the thickness. This effect is due to an overpressure in the film, which is caused by the interaction of the two highly ordered surface layers. In several studies [4–6] Landau models have been developed, which describe the dependence on the thickness very well. However, the temperature dependence of this effect is only predicted qualitatively. Probably the experimental conditions for application of these models are not suitable. First, Landau–de Gennes theories can only be used in a limited temperature region around a transition point and our measurements extend up to 15 K below the N-A transition point. Second, the thinnest films studied show a thickness of about 6 nm, which is of the order of the coherence length. This should also lead to artifacts in the Landau–de Gennes theory.

Furthermore, we have used the mean field theories of McMillan [22,23] modified by Mirantsev [24] and Kranjc and Zumer [25] to describe smectic films. Their theories have been adapted by us to investigate the film tension. We were not able to describe the temperature dependence of the film tension in ultrathin films with physically reasonable parameters, although the theory allows, in general, to study a broader range of properties.

ACKNOWLEDGMENTS

Financial support by the Deutsche Forschungsgemeinschaft is gratefully appreciated.

[1] P. Pieranski *et al.*, Physica A **194**, 364 (1993).
[2] J.-C. Géminard, R. Holyst, and P. Oswald, Phys. Rev. Lett. **78**, 1924 (1997).
[3] F. Picano, R. Holyst, and P. Oswald, Phys. Rev. E **62**, 3747 (2000).
[4] F. Picano, P. Oswald, and E. Kats, Phys. Rev. E **63**, 021705 (2001).
[5] A.N. Shalaginov and D.E. Sullivan, Phys. Rev. E **63**, 031704 (2001).
[6] A. Poniewierski, P. Oswald, and R. Holyst, Langmuir **18**, 1511 (2002).
[7] T. Stoebe, P. Mach, and C.C. Huang, Phys. Rev. E **49**, R3587 (1994).
[8] P. Mach, S. Grantz, D.A. Debe, T. Stoebe, and C.C. Huang, J. Phys. II **5**, 217 (1995).
[9] T. Stoebe, P. Mach, S. Grantz, and C.C. Huang, Phys. Rev. E **53**, 1662 (1996).
[10] P.M. Johnson, P. Mach, E.D. Wedell, F. Lintgen, M. Neubert, and C.C. Huang, Phys. Rev. E **55**, 4386 (1997).
[11] P. Mach, S. Grantz, T. Stoebe, and C.C. Huang, Mol. Cryst. Liq. Cryst. Sci. Technol., Sect. A **302**, 181 (1997).
[12] R. Stannarius and C. Cramer, Europhys. Lett. **42**, 43 (1998).
[13] F. Schneider, Rev. Sci. Instrum. **73**, 114 (2002).
[14] C. Rosenblatt and N.M. Amer, Appl. Phys. Lett. **36**, 432 (1980).
[15] E.B. Sirota, P.S. Pershan, L.B. Sorensen, and J. Collett, Phys. Rev. A **36**, 2890 (1987).
[16] I. Kraus, P. Pieranski, E. Demikhov, H. Stegemeyer, and J. Goodby, Phys. Rev. E **48**, 1916 (1993).
[17] S.-T. Wu, C.-S. Wu, M. Warenghem, and M. Ismaili, Opt. Eng. **32**, 1775 (1993).
[18] A.J. Leadbetter, J.C. Frost, J.P. Gaughan, G.W. Gray, and A. Mosley, J. Phys. (Paris) **40**, 375 (1979).
[19] A. Ajdari, L. Peliti, and J. Prost, Phys. Rev. Lett. **66**, 1481 (1991).
[20] A. Ajdari, B. Duplantier, D. Hone, L. Peliti, and J. Prost, J. Phys. II **2**, 487 (1992).
[21] W.H. Press, S.A. Teukolsky, W.T. Vetterling, and B.P. Flannery, *Numerical Recipes in Fortran*, *The Art of Scientific Computing* (Cambridge University Press, Cambridge, 1994).
[22] W.L. McMillan, Phys. Rev. A **4**, 1238 (1971).
[23] W.L. McMillan, Phys. Rev. A **6**, 936 (1972).
[24] L.V. Mirantsev, Phys. Lett. A **205**, 412 (1995).
[25] T. Kranjc and S. Zumer, Mol. Cryst. Liq. Cryst. Sci. Technol., Sect. A **304**, 295 (1997).